

See discussions, stats, and author profiles for this publication at: <https://www.researchgate.net/publication/281261244>

Super Toughened Biobased Poly(Lactic Acid)/Epoxidized Natural Rubber Thermoplastic Vulcanizates: Fabrication, Co-Continuous Phase Structure, Interfacial In-situ Compatibilization a...

ARTICLE *in* THE JOURNAL OF PHYSICAL CHEMISTRY B · AUGUST 2015

Impact Factor: 3.3 · DOI: 10.1021/acs.jpcb.5b06244 · Source: PubMed

READS

27

4 AUTHORS, INCLUDING:



Chuanhui Xu

Guangxi University

44 PUBLICATIONS 244 CITATIONS

[SEE PROFILE](#)



Yukun Chen

South China University of Technology

47 PUBLICATIONS 248 CITATIONS

[SEE PROFILE](#)

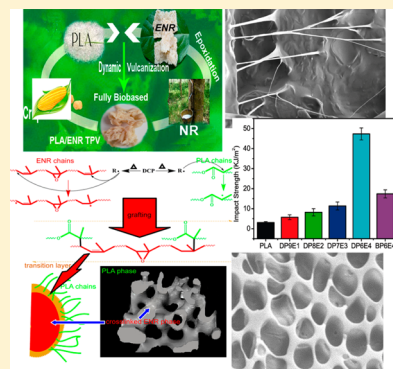
Supertoughened Biobased Poly(lactic acid)–Epoxidized Natural Rubber Thermoplastic Vulcanizates: Fabrication, Co-continuous Phase Structure, Interfacial in Situ Compatibilization, and Toughening Mechanism

Youhong Wang,[†] Kunling Chen,[†] Chuanhui Xu,^{*,†,‡} and Yukun Chen^{*,†}

[†]The Key Laboratory of Polymer Processing Engineering, Ministry of Education, South China University of Technology, Guangzhou, 510640 China

[‡]School of Chemistry and Chemical Engineering, Guangxi University, Nanning, 530004 China

ABSTRACT: In the presence of dicumyl peroxide (DCP), biobased thermoplastic vulcanizates (TPVs) composed of poly(lactic acid) (PLA) and epoxidized natural rubber (ENR) were prepared through dynamic vulcanization. Interfacial in situ compatibilization between PLA and ENR phases was confirmed by Fourier transform infrared spectroscopy (FT-IR). A novel “sea–sea” co-continuous phase in the PLA/ENR TPVs was observed through scanning electron microscopy (SEM) and differed from the typical “sea–island” morphology that cross-linked rubber particles dispersed in plastic matrix. A sharp, brittle–ductile transition occurred with 40 wt % of ENR, showing a significantly improved impact strength of 47 kJ/m², nearly 15 times that of the neat PLA and 2.6 times that of the simple blend with the same PLA/ENR ratio. Gel permeation chromatography (GPC) and dynamic mechanical analysis (DMA) results suggested that a certain amount of DCP was consumed in the PLA phase, causing a slight cross-linking or branching of PLA molecules. The effects of various DCP contents on the impact property were investigated. The toughening mechanism under impact testing was researched, and the influence factors for toughening were discussed.



1. INTRODUCTION

Given the increasing awareness of environmental protection and energy crises, biodegradable and biobased polymers are of growing consideration in both academic research and industrial applications.^{1,2} Poly(lactic acid) (PLA) has become one of the brilliant stars in various eco-friendly polymers because of its competitive price and high strength as well as being renewable and degradable.^{3,4} However, neat PLA cannot meet the requirements in some special circumstances because of its natural brittleness; thus, a toughening modification has been a PLA-based material science issue for decades and still has a powerful attraction.⁵

Blending with a second elastomeric component to enhance the ductility of PLA is an economic and practical method. However, simple blending without any physical or chemical interactions between rubber and plastic seems not very ideal for achieving the anticipated properties.^{6–8} Reactive blending to initiate in situ interfacial compatibilization between PLA and the rubbers during blending is an efficient way to improve the impact strength of PLA.^{9–11} Among the various reactive blending methods, the dynamic vulcanizing technique, a process of selectively vulcanizing the rubber phase in the presence of a cross-linking agent under shearing and the desired temperature,^{12–14} has been broadly employed to fabricate toughened blends, e.g., the polypropylene/ethylene-propylene-diene monomer (PP-/EPDM), a classical case when it

comes to thermoplastic vulcanizates (TPVs). On this basis, a variety of elastomers have been blended with PLA. Lu et al.¹⁵ reported a toughened PLA by in situ reactive interfacial compatibilization via dynamically vulcanizing polyurethane elastomer prepolymer. Liu et al.¹⁶ reported a PLA ternary blend with high impact toughness prepared by melt-blending PLA with elastomeric ethylene-*n*-butyl acrylate-glycidyl methacrylate (EBA-GMA) and a zinc ionomer of ethylene-methacrylic acid (EMAA-Zn) copolymer. EBA-GMA was dynamically vulcanized in the presence of EMAA-Zn. Wang et al.¹⁷ reported a supertoughened PLA modified by an unsaturated aliphatic polyester elastomer (UPE). Dynamic vulcanization of UPE occurred in the presence of dicumyl peroxide (DCP) as an initiator. Ma et al.¹⁸ recently applied the dynamic vulcanization method to prepare PLA/ethylene-*co*-vinyl acetate (EVA) TPVs with high strength and elongation at break, moderate hardness, and a low tensile set. Thermoplastic polyurethane (TPU),¹⁹ poly(ethylene-glycidyl methacrylate) (EGMA),²⁰ thermoplastic elastomer poly(ester-amide) (PEA),²¹ and biobased polyester elastomer (BPE)²² were also reported to modify PLA. Although these elastomers did good

Received: June 30, 2015

Revised: August 17, 2015

Published: August 24, 2015

jobs at toughening PLA, most of them are synthetic or petroleum-based materials.

As a renewable resource with high elasticity, natural rubber is a competitive toughener for PLA.^{23–26} Bitinis et al.^{23,24} reported a lot of works on the physical blending of PLA/NR in which they suggested that ~10 wt % of NR got the best balanced properties. Considering the great polarity difference of NR and PLA, enormous efforts have also been made to improve their compatibility. Chumeka et al.,²⁷ Jaratrotkamjorn et al.,²⁸ and Juntuek et al.²⁹ incorporated compatibilizers of NR-g-(vinyl acetate) (VA), NR-g-(methyl methacrylate) (MMA), and NR-g-(glycidyl methacrylate) (GMA) into PLA/NR blends, respectively. Epoxidized natural rubber (ENR), derived from natural rubber latex after being treated with peroxide,³⁰ has better compatibility with PLA. However, there are only a few examples of literature^{31–33} reported using ENR to modify PLA. Zhang et al.³¹ studied the simple blending of PLA with ENR20 and ENR50, reporting that ENR20 showed a better toughening effect than did ENR50. Akbari et al.³² investigated ENR-toughened PLA/talc composites and reported that the blending of ENR50 (20 wt %) to PLA/talc (30 wt %) revealed a significant improvement (448%) of impact strength, with a considerable sacrifice in Young's and flexural modulus. To the best of our knowledge, no reports have been involved in dynamic vulcanization with an *in situ* reaction to prepare ENR-toughened PLA TPVs.

In our previous study of a dynamically vulcanized PLA/NR system,²⁶ we found that the cross-linked NR was a continuous phase rather than dispersed particles. The dynamically vulcanized PLA/NR system with this novel phase structure exhibited supertoughness. In this paper, NR was replaced by ENR, and the preparation, compatibilization, morphology, mechanical properties, and toughening mechanism of biobased PLA/ENR TPVs were reported. The novel co-continuous phase structure was also found in the PLA/ENR system. In addition, dynamic vulcanization of ENR and interfacial compatibilization also took place through the reaction of PLA with ENR in the presence of dicumyl peroxide as an initiator. The impact toughness of PLA was improved significantly by the *in situ* compatibilization and the novel co-continuous phase morphology. With significantly improved toughness, the biobased PLA/ENR TPV was a potential alternative to replace some petroleum-based commodity plastics. We also hope that this paper may enrich and contribute to this new finding of co-continuous phase structure as well as toughening PLA.

2. EXPERIMENTS AND METHODS

2.1. Materials. PLA (grade REVOODE110), with a weight-average molecular weight (M_w) of 1.7×10^5 g/mol, MI (190 °C, 2.16 kg) of 2–10 g/10 min, and density of 1.25 g/cm³, was purchased from Zhejiang Hisun Biomaterials Co., Ltd. ENR with 30 mol % of epoxidation was kindly provided by the Chinese Academy of Tropical Agricultural Sciences. DCP used in this work was recrystallized by anhydrous alcohol before use and obtained from Sinopharm Chemical Reagent Co. Ltd. (Shanghai, China). Irganox 1010 antioxidant (industrial grade) was commercially available. The other chemicals were used as received.

2.2. Preparation of Dynamically Vulcanized PLA/ENR TPVs. Before being processed, PLA was dried for 6 h in a vacuum oven at 80 °C to remove the moisture, and ENR was masticated. The dynamically vulcanized PLA/ENR TPVs with different weigh ratio (90/10, 80/20, 70/30, and 60 wt% /40 wt

%) were fabricated in a Haake Rheometer (Haake Rheomix 600,) at a rotor speed of 60 rpm and a set temperature of 150 °C. In this particular experiment, the DCP loading was fixed at 1.5 wt % of the ENR phase; therefore, the actual dosage of DCP was various according to different PLA/ENR ratios. The specific procedures are as follows.

First, PLA with 0.2 wt % of Irganox 1010 was premixed in the chamber. After reaching a stable torque, the masticated ENR was incorporated. About 3 min later, DCP was added to initiate the dynamic vulcanization of ENR, which was continued for another 3 min. Subsequently, the hot resultants were removed from the cavity and cooled to room temperature. Then, the cooled TPVs were chopped into small granules for injection molding in a TTI-160F (Welltec Machinery Co. Ltd., Hong Kong, China). The nozzle temperature was 175 °C, and the dies were at room temperature. The injection pressure was set as 40 MPa.

For brevity, the sample codes were named according to the PLA/ENR ratio, e.g., the dynamically vulcanized PLA/ENR (80/20) TPV was defined as DP8E2. Simple blends of PLA/ENR (80/20) were named BP8E2.

2.3. Mechanical Property Measurements. Tensile strength and elongation at break of the dumbbell-shaped specimens were measured on a universal testing instrument (Tensile mold, Shimadzu AG-1, 10 KG) at a testing speed of 50 mm/min according to ISO 527-2 at room temperature. Notched Izod impact testing was performed in a ZWICK5331 (Zwick/Roell) testing machine at room temperature, and the sample bars were of 2 mm depth and a 45° angle according to ISO 180.

2.4. Fourier Transform Infrared Spectroscopy. Next, Fourier transform infrared spectroscopy (FT-IR) was performed on a Tensor 27 spectrometer (Bruker). The absorption spectra were recorded with a resolution of 4 cm⁻¹ and 32 scans in the waves number range from 400 to 4000 cm⁻¹. The neat PLA and ENR sheets were directly used for FT-IR testing with a attenuated total reflectance (ATR) model. For PLA/ENR TPVs, ~4 g of small granules were first extracted with dichloromethane (DCM) in a Soxhlet extraction apparatus at 40 °C for 72 h to selectively get rid of free PLA. Then, the residuals were dried in a vacuum oven at 60 °C until a constant weight was reached to eliminate the effect of residual solvent and moisture before testing. Finally, thin films were made with the dried insoluble residues and used for FI-TR tests with an ATR model.

2.5. Dynamic Mechanical Analysis. Dynamic mechanical properties of the PLA/ENR TPVs were measured with DMA 242C (NETZSCH) in a tensile mode with an oscillation frequency of 1 Hz. The samples, obtained from molding, were taken from -100 to 120 °C at a heating rate of 3 °C/min.

2.6. Apparent Cross-Link Density of the ENR Phase. It has been widely recognized that the volume fraction of the rubber phase when swollen in the sample gel could be used for the cross-link density.^{34–37} All of the specimens with a size of 7 × 7 × 2 mm were weighed and then immersed in toluene at an ambient temperature until swelling equilibrium was achieved. After that, the swollen samples were taken out and blotted with filter paper to remove the external solvent. Immediately after that, the samples were weighed again on an analytical balance, and the apparent cross-link density was calculated by the following equation.^{34–36}

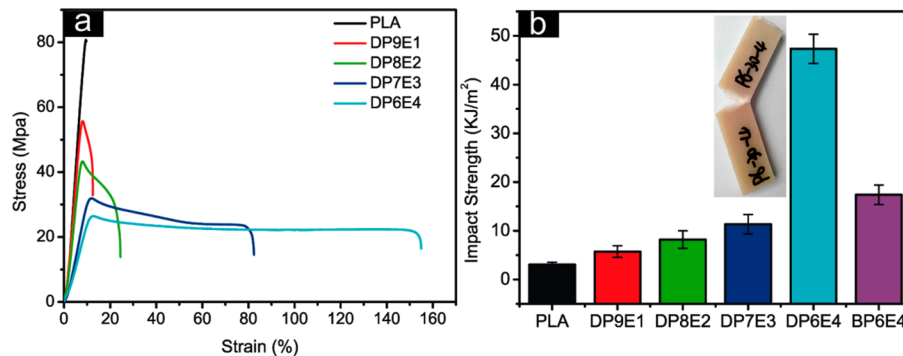


Figure 1. Mechanical properties of neat PLA and PLA/ENR TPVs with different PLA/ENR weight ratios: (a) stress–strain curves and (b) notched Izod impact strength.

$$V_r = \frac{1}{1 + \left(\frac{m_2}{m_1} - 1 \right) \times \frac{\rho_t}{\alpha \rho_s}} \quad (1)$$

where m_1 and m_2 are the total mass of the sample before and after swelling; ρ_r and ρ_s represent the ENR and toluene density ($\rho_s = 0.865 \text{ g/cm}^3$), respectively; and α is the weight content of ENR in the sample.

2.7. Scanning Electron Microscopy. Merlin field emission scanning electron microscopy (FE-SEM, Carl Zeiss) was used to observe the morphology of PLA/ENR TPVs. Prior to fractographic examination, all specimens were pasted on an aluminum stub using a conductive paint and sputter-coated with gold to prevent electrostatic charge build-up during observation.

2.8. Gel Permeation Chromatography. A EC2000 gel permeation chromatograph (Dalian Elite Analytical Instruments Co. Ltd., Dalian, China) with a Shodex GPC column (K-804L) was used to investigate the variation of molecular weight and molecular weight distribution (poly dispersity index (PDI)) for neat PLA and PLA component from the TPVs. First, about 3 g of sample was dissolved in 5 mL of chloroform, the suspension was filtered to remove ENR residues, and then the obtained clear solution was precipitated in excessive cold methanol. Second, the PLA precipitates were dried at 60 °C on a vacuum oven to a constant weight for gas permeation chromatography (GPC) analysis. Chloroform was used as the elution solvent at a flow rate of 1.0 mL/min; the concentration of PLA in chloroform was 10 mg/mL and injected by 50 μL increments at room temperature.

3. RESULTS AND DISCUSSION

3.1. Mechanical Properties. The tensile behaviors and impact strengths of neat PLA and PLA/ENR TPVs are first shown in Figure 1. As seen from Figure 1a, the stress–strain curve of neat PLA showed a typical brittle fracture with a tensile strength and an elongation at break of 81.4 MPa and ~9.5%, respectively, while the PLA/ENR TPVs displayed an apparent yielding characteristic with a feature of improved ductile fracture. Because the ENR with a much lower modulus was incorporated into PLA matrix, the stress–strain curves of the TPVs showed a decreasing tensile strength maximum (yielding stress). This led to an inevitable sacrifice of 30–67% in tensile strength of the PLA with the incorporation of 10–40 wt % ENR. It was noteworthy that the DP6E4 (with ~40 wt % ENR) and the DP7E3 (with ~30 wt % ENR) showed an inconspicuous decrease of stress after yielding compared with

that of the DP8E2 (with ~20 wt % ENR) and the DP9E1 (with ~10 wt % ENR), presenting typical tensile behavior of polymer blends with an improved interfacial compatibility.^{24,38} The elongation at break, showing the same trend with impact strength (Figure 1b), increased with the increasing content of ENR. The DP6E4 displayed the highest strain value of ~150%, almost 16 times higher than that of the neat PLA (~9.5%). The similar ductile behavior could be found in most plastic blended with a high content of rubbers.^{15,39} As shown in Figure 1b, a remarkable brittle–ductile transition was achieved in the DP6E4, which showed an impact strength of 47 kJ/m², nearly 15 times that of the neat PLA (3 kJ/m²) and ~2.6 times that of the BP6E4 (18.2 kJ/m²). It should be noted that all of the test specimens of DP6E4 were not completely fractured, as exhibited in the inset picture of Figure 1b. Further increasing the ENR phase (e.g., 50 wt % of ENR) resulted in a supertoughened PLA/ENR TPV. However, impact testing for this sample failed because all of the specimens of DPSE5 slipped without any surface-breaking cracks when they were impacted by the cantilever beam (not shown here).

3.2. Co-continuous Phase Structure in PLA/ENR TPVs.

The cryogenically fractured surface was obtained after the samples were fully frozen in liquid nitrogen. Figure 2a,b

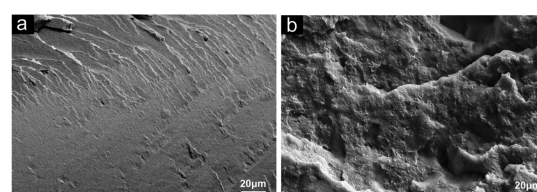


Figure 2. SEM images of cryogenically fractured surfaces of (a) neat PLA and (b) DP6E4.

displays the SEM images of cryogenically fractured surfaces of neat PLA and DP6E4, respectively. Obviously, the neat PLA showed a relatively smooth surface and typical brittle fracture with no plastic deformation. As expected, DP6E4 showed a very coarse surface with typical toughening characteristics. Although it is not possible to distinguish the PLA phase and ENR phase from Figure 2b, the obscure phase boundary could be confirmed, and no “pulling out” phenomenon of the ENR phase was observed on the cross-sections of the DP6E4, implying a superior compatibility between the two phases.¹⁹ This is consistent with the FT-IR results, which will be discussed later. It has been widely reported that phase morphology, especially the soft phase, has a significant effect

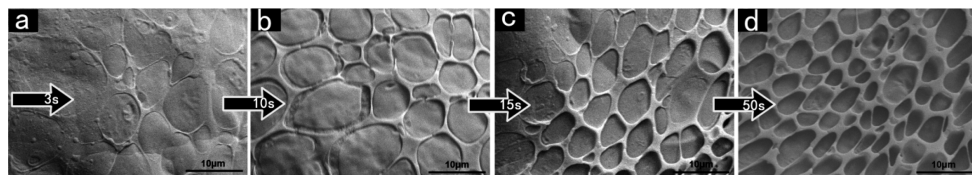


Figure 3. SEM images of cryogenically fractured surfaces of DP6E4 (PLA/ENR = 60:40) etched by DCM for (a) 3, (b) 10, (c) 15, and (d) 50 s at room temperature.

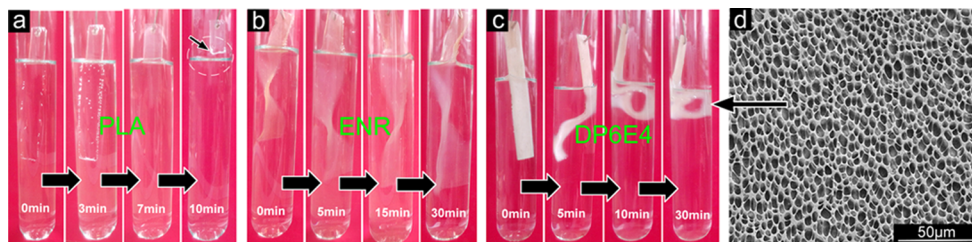


Figure 4. Photographs of swelling experiments for (a) PLA, (b) ENR, and (c) DP6E4. (d) Netlike phase structure of ENR in DP6E4.

on impact properties of a toughened blend.⁴⁰ To further explore the phase structure of the ENR phase, we used DCM to etch the PLA continuous phase. However, the soft nature of the ENR phase inevitably made it collapse or shrink without the support of the rigid PLA phase. To solve this issue, we controlled the etching time carefully to remove the PLA on the cryogenically fractured surface of the DP6E4 with layer-by-layer stripping. The results of this processing are shown in Figure 3. Similar to that of the PLA/NR system, which we reported previously,³⁹ the netlike continuous phase structure of the ENR was gradually exposed after layer-by-layer stripping of the PLA phase (PLA/ENR = 60:40). It was clearly seen that the slight shrinkage of the netlike phase structure of the ENR in Figure 3d. To further confirm the continuous ENR phase, we here also show the swelling experiments results of PLA, ENR, and DP6E4 in Figure 4, respectively. As can be seen, PLA was dissolved completely in DCM within 10 min (Figure 4a), but ENR was only swollen (Figure 4b). DP6E4 did not dissolve but only crimped after the PLA phase was dissolved (Figure 4c). This strongly confirmed that the ENR phase was a continuous structure in the PLA. Figure 4d also shows a netlike phase structure of ENR in DP6E4 at a lower amplification. This implied that the continuous ENR phase had a significantly elastic structure that functioned as a toughening framework throughout the PLA matrix. Deformation of the ENR with this novel netlike phase structure absorbed more energy, contributing to the high toughness of the blend system.

3.3. Dynamic Cross-Linking of the ENR Phase and in Situ Interfacial Compatibilization. Figure 5 presents the evolution of torque with time during the entire processing of dynamic vulcanization. The first two larger melt torque peaks were attributed to the melting of PLA and ENR, respectively. The maximum torques values of the PLA and ENR components corresponded to their respective concentrations in TPVs. For all TPVs, the torque showed a detectable rise after the addition of DCP, confirming the occurrence of vulcanization of the ENR phase.¹⁴ Additionally, the slope of cross-linking torque curve increased with the ENR content, suggesting a faster vulcanization at higher ENR/PLA ratios. After going through a maximum, the torque decreased slightly until it reached a new equilibrium platform at the end of mixing, implying the full final vulcanization of the ENR phase.

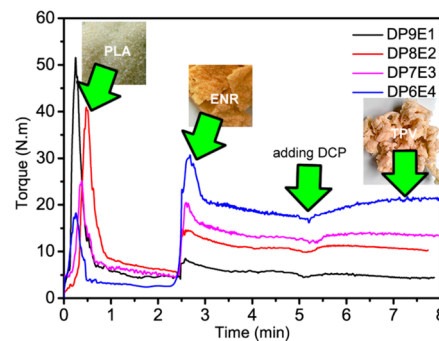


Figure 5. Melt torque versus processing time for PLA/ENR TPVs.

It must be pointed out that the actual temperature would be higher ($\sim 158\text{--}160\text{ }^{\circ}\text{C}$) than the set temperature ($150\text{ }^{\circ}\text{C}$) after the ENR was added because the shearing and friction between materials (particularly the ENR) and rotors will generate a great deal of heat in a confined chamber.⁴¹ The additional friction heat promoted the vulcanization of the ENR phase. The inset digital picture of TPV in Figure 5 shows the appearance of the DP6E4 after cooling from the chamber. It was clearly seen that the TPV was an integral material without phase separation, suggesting that a considerable interfacial compatibility between PLA and ENR was achieved.

It is well-known that compatibility of blends plays a very important role in improving the mechanical properties of the blend materials.¹² Sufficient interfacial adhesion facilitates stress transference from the rigid plastic phase to the soft rubber phase, which could effectively prevent the cracks initiated at the phase interface from growing to catastrophic failure.^{17,38} To confirm that the in situ reactive compatibilization of the PLA and ENR occurred during DCP-induced dynamic vulcanization, we employed FT-IR to quantitatively investigate the interface-grafting reaction. Figure 6a shows the absorption spectra of the neat PLA, ENR, and DCM-extracted DP8E2, DP7E3, and DP6E4 in the range of $800\text{--}1900\text{ cm}^{-1}$. As for the PLA, the characteristic absorption peak at 1750 cm^{-1} corresponded to the stretching vibration of carbonyl groups ($\text{C}=\text{O}$) in the PLA molecule.^{10,39,42} The FT-IR spectra of the ENR clearly showed its characteristic absorption peaks at 870 and 1375 cm^{-1} , which were related to the antisymmetric stretching vibration of the

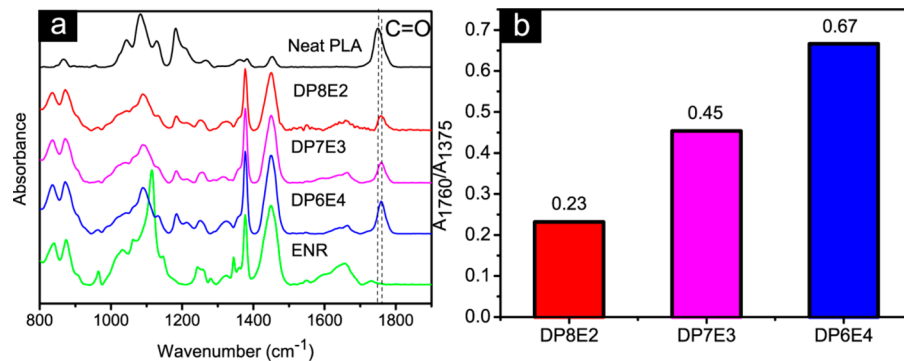


Figure 6. (a) FT-IR absorption spectra and (b) the ratio of absorption peak area (A_{1760}/A_{1375}) of DP8E2, DP7E3, and DP6E4.

epoxy group and the symmetric stretching deformation of methyl ($-\text{CH}_3$),⁴³ respectively. The spectra of the insoluble residues of DCM-extracted DP8E2, DP7E3, and DP6E4 were almost parallel to that of the neat ENR, which suggested the complete elimination of the free PLA after extraction by DCM for 4 days. As expected, compared to those of the neat ENR, the residues of DCM-extracted samples showed a new absorption with a different intensity at 1760 cm^{-1} , suggesting that the PLA was grafted onto the ENR molecular during the dynamic vulcanization. The PLA molecule chains were possibly initiated to form active points (e.g., tertiary carbon free radicals) through the DCP radical-seizing hydrogen atom,^{17,44} which reacted with the ENR (or ENR radicals), forming PLA-g-ENR graft copolymers at the interface of PLA and ENR. Additionally, the new absorption peak representing C=O stretching was shifted to a higher wavenumber, from 1750 cm^{-1} (as the dash line showed), which further confirmed the chemical interaction between the PLA and ENR.³³ The detailed information for interface reaction can be approximately described by the molar ratio of the PLA repeat unit in the insoluble residues, as is calculated by the ratio of absorption peak area at 1760 cm^{-1} to that at 1375 cm^{-1} (A_{1760}/A_{1375} , where A_{1760} and A_{1375} are the peak areas of 1760 and 1375 cm^{-1} , respectively). The calculated results of the A_{1760}/A_{1375} are shown in Figure 6b. The value of A_{1760}/A_{1375} was increased as the weight ratio of ENR increased. This was due to the fact that the increased actual dosage of DCP generated more macromolecular radicals of PLA and ENR to form grafting copolymers. Consequently, a stronger interface (transition layer) was achieved in a TPV with higher ENR content, which offered synergistic or additive action on toughening PLA. On the basis of the above analysis, the possible in situ compatibilization and the transition layer at the interface between PLA and ENR phases are illustrated in Figure 7.

3.4. Dynamic mechanical behavior. Figure 8a represents the tangent of δ as a function of temperature for neat PLA, vulcanized ENR (cured with 1.5 wt % of DCP), and PLA/ENR TPVs. Two $\tan \delta$ peaks at around -20 and $65\text{ }^\circ\text{C}$ ^{18,39} corresponded to the glass transition of ENR and PLA, respectively. It was noted that the $\tan \delta$ peak temperatures of the ENR phase in TPVs presented a lower glass transition temperature ($-22.46\text{ }^\circ\text{C}$ for DP6E4, $-23.35\text{ }^\circ\text{C}$ for DP7E3, and $-23.82\text{ }^\circ\text{C}$ for DP8E2) than the vulcanized pure ENR ($-19.87\text{ }^\circ\text{C}$). Similarly, the $\tan \delta$ peak temperatures of the PLA phase in TPVs also shifted to lower temperature ($62.25\text{ }^\circ\text{C}$ for DP6E4, $63.82\text{ }^\circ\text{C}$ for DP7E3, and $64.78\text{ }^\circ\text{C}$ for DP8E2) than the neat PLA ($65.02\text{ }^\circ\text{C}$). The above changes in $\tan \delta$ peak

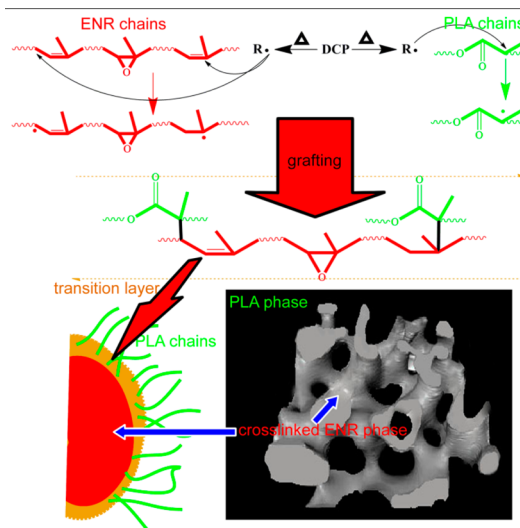


Figure 7. Scheme of possible in situ compatibilization and the transition layer at the interface between PLA and ENR phases.

temperatures were attributed to the actual dosage of effective DCP functioned in different phases. In this particular experiment, the actual dosage of DCP varied according to different PLA/ENR ratios because the DCP loading was fixed at 1.5 wt % of the ENR phase. The PLA phase in TPVs also consumed partial DCP, reducing the actual DCP as cross-linking agent for the ENR phase. At a higher ENR/PLA ratio, more DCP was added, which promoted the contact chance with the PLA phase and the ENR phase. This resulted in a higher cross-link density of the ENR phase (see Figure 9) and hence a higher glass transition temperature.⁴⁵ However, more DCP was also consumed in the PLA phase, generating slight cross-linking or branching of PLA molecules.^{18,42} The slight cross-linking (not forming a network) or branching could interfere with the ordered arrangement of polymer chains and thus provide more free volume for chains. This increased the distance between molecules and enhanced the segmental activity of PLA, resulting in a lower glass transition temperature. We believed that the slight cross-linking or branching of PLA molecules also contributed to the toughening of PLA. The storage modulus dependence on temperature was consistent with the $\tan \delta$, as displayed in Figure 8b; a sharp decline of storage modulus for neat PLA at about 50 to $80\text{ }^\circ\text{C}$ and ENR at about -30 to $0\text{ }^\circ\text{C}$ were observed, owing to their glass transition. The incorporation of ENR with a soft nature

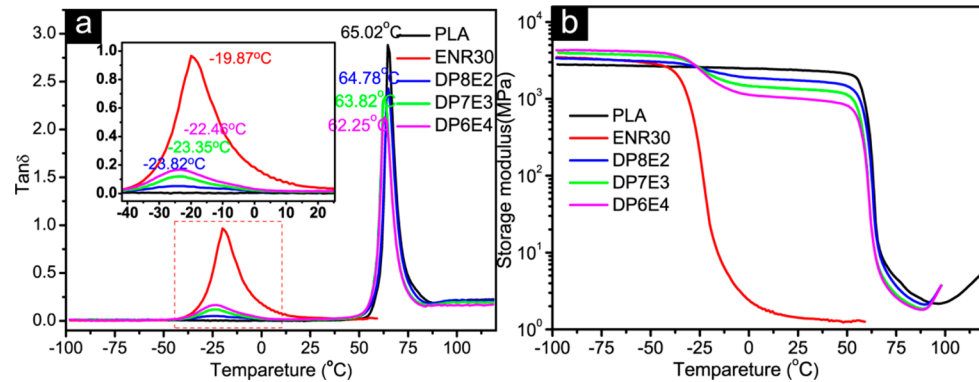


Figure 8. (a) Values for $\tan \delta$ as a function of temperature; (b) storage modulus as a function of temperature.

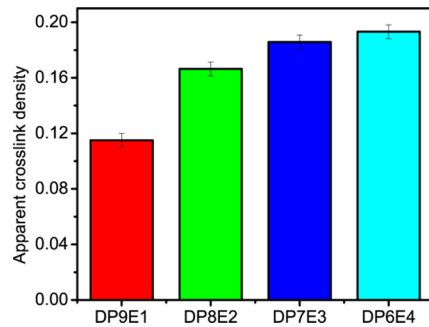


Figure 9. Cross-link density of the ENR phase in PLA/ENR TPVs.

decreased the storage modulus of the PLA, exhibiting a toughening effect.

3.5. Effect of DCP on the PLA Phase. To confirm the influence of DCP on the PLA phase, we designed a comparison experiment with the molecular weight and distribution of the neat PLA; the neat PLA (melted) mixed at 160 °C for 8 min, the PLA with 0.4 wt % DCP mixed at 160 °C for 8 min, and PLA in DP8E2 was determined by GPC, as shown in Figure 10.

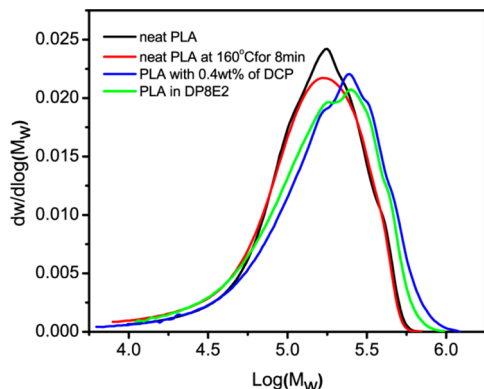


Figure 10. Molecular weight distribution of the PLA and PLA phases in DP8E2.

Molecular weight parameters of the above samples are summarized in Table 1. As expected, the M_w of PLA was 176 739 g/mol, and the M_w of the PLA phase in DP8E3 was increased to 202 903 g/mol. The DCP initiated the chemical reaction of PLA molecules during dynamic vulcanization and resulted in an increased molecular weight and a slightly broad molecular weight distribution, which suggested that the degradation⁴⁶ and slight cross-linking or branching of PLA

Table 1. Molecular Weights of PLA and PLA Phases in DP8E2

sample	M_n (g/mol)	M_w (g/mol)	M_p (g/mol)	$PDI(M_w/M_n)$
neat PLA	106 111	176 739	176 405.02	1.67
PLA, 160 °C	91 960	170 541	165 991.1	1.85
PLA, 0.4 wt % DCP	109 846	226 478	242 198.8	2.06
PLA in DP8E2	106 712.8	202 903	249 857.5	1.9

molecules took place simultaneously during DCP-induced dynamic vulcanization. The GPC results were consistent with the previous analysis of the dynamic mechanical analysis results that the $\tan \delta$ peak temperatures of the PLA phase in TPVs shifted to lower temperatures.

3.6. Toughening Mechanism. The impact fracture surface obtained from the notched Izod impact test was also characterized by SEM. Figure 11 shows the SEM micrographs

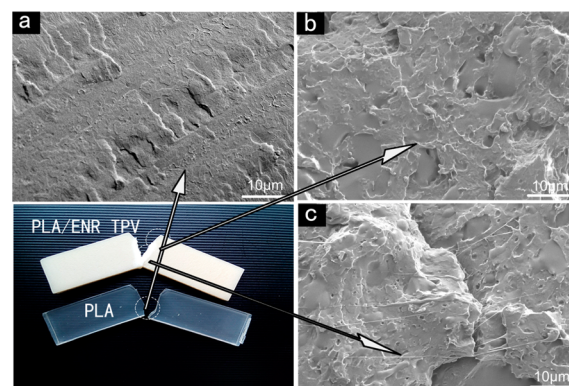


Figure 11. SEM micrographs for the impact fractured surfaces of (a) neat PLA; (b) DP6E4, near the initial impact section; and (c) DP6E4, near the unbroken section.

for the impact-fractured surfaces of neat PLA and the typical PLA/ENR TPVs (DP6E4). As shown in Figure 11a, the neat PLA showed a typical brittle fracture surface with no stress-whitening zones and fibrils. To study the toughening mechanism of the PLA/ENR TPVs, we selected different locations of the impact-fractured surfaces for SEM observation. Because the unbroken section (point) was quite uneven, the SEM observation was difficult to conduct. Therefore, we selected an observation point that was a 1–2 mm distance to the unbroken point. The results are shown in Figure 11b,c. With the incorporation of ENR, TPV showed a rougher surface

with obvious plastic deformation, suggesting a typical toughening fracture. No voids resulting from “pulling out” were observed in Figure 11b, indicating that the cross-linked netlike ENR phase was very compatible with the PLA matrix. As shown in Figure 11c, the observation point was near the unbroken section, and denser plastic deformation was further evidenced by the appearance of elastic microfibrils. There was no doubt that the formation of microfibrils absorbed more impacting energy and resulted in rougher morphologies, consequently improving impact strengths.^{16,39} Because of its rigid and brittle nature, PLA was unable to be elongated to form elastic microfibrils. Therefore, the observed elastic microfibrils were resulted from the highly elongated netlike ENR continuous phase, which is shown in Figure 3. We believed this novel netlike continuous phase structure had a more effective toughening effect than did the conventional rubber particles on the PLA.

Figure 12a shows the detailed morphology structure of the ENR microfibrils. The elastic nature of the microfibrils was

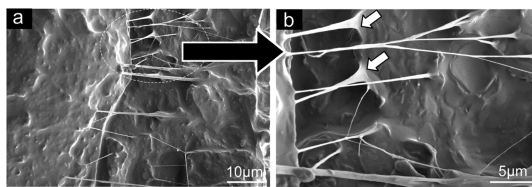


Figure 12. (a) Morphology structure of the ENR microfibrils, $\times 2000$; (b) detailed morphology structure of the ENR microfibrils, $\times 5000$.

visualized in Figure 12b with a higher-magnification SEM image. It should be noted that the root parts of the elongated ENR microfibrils were firmly bonded with the TPV matrix without any viewable cracks, again confirming the excellent interfacial adhesion between the ENR phase and the PLA phase. This was consistent with the FT-IR analysis that the in situ compatibilization and the transition layer at the interface between the PLA and ENR phases significantly improved interfacial adhesion. It is well-known that the effectiveness of a selected rubber toughened plastics system is mainly determined by the blend ratio of rubber, the size and shape of the rubber phase, and the interfacial adhesion between rubber and plastic, etc.³¹ During the fracturing process, the fracture crack progressed along the interface, and the crack energy was absorbed and dissipated by the soft rubber phase, avoiding brittle breaking. However, as shown in Figure 3, there were no dispersed particles formed in this particular PLA/ENR system. Additionally, no cracks (but only microfibrils) appeared on the impact fractured surfaces of the PLA/ENR TPV. In this regard, the novel netlike ENR continuous phase structure and the compatibility between ENR and PLA were the main effective factors. During the fracturing process of PLA/ENR TPVs, the PLA phase (slightly cross-linked or branched) ruptured first, accompanied by improved plastic deformation. The netlike ENR continuous phase at the rupture opening was elongated until it broke or formed microfibrils; this process absorbed a lot of impact energy. The interfacial adhesion transferred the impact energy effectively from the PLA phase to the ENR phase, further assisting the dissipation of energy. As a result, a further enhancement of impact strength occurred when the higher rubber content was added due to the fact that more acceptors of the dissipation energy formed.

It is more attractive to study the effect of DCP dosage on the impact fractured surfaces of TPVs. The SEM micrographs for the impact-fractured surfaces of PLA/ENR TPVs with various DCP dosages are shown in Figure 13a–d. Rougher

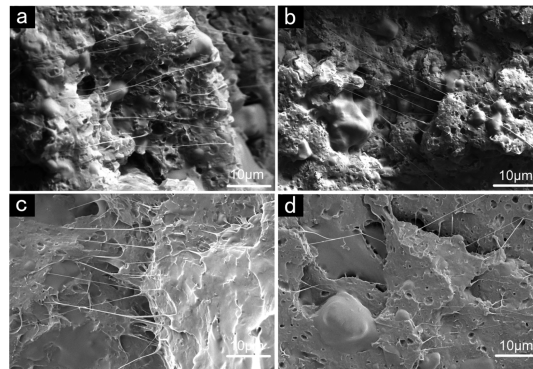


Figure 13. Impact fractured surfaces of PLA/ENR TPVs with various DCP dosages: (a) 0.5 wt % of the ENR phase (TPV-0.5); (b) 1.0 wt % of the ENR phase (TPV-1.0); (c) 1.5 wt % of the ENR phase (TPV-1.5); and (d) 2.0 wt % of the ENR phase (TPV-2.0).

morphologies with increased microfibrils and plastic deformations with increased DCP dosages were observed in Figure 13a–c, corresponding to enhanced impact strength from 36 kJ/m² for TPV-0.5 to 41 kJ/m² for TPV-1.0 and 47 kJ/m² for TPV-1.5. However, when the DCP content increased to 2 wt % of the ENR phase, the impact strength showed a slight decrease to 45 kJ/m². As seen from Figure 13d, an apparent reduction of microfibrils and plastic deformations can be observed. Although the interfacial compatibility between PLA and ENR was further improved at a higher DCP content, the simultaneous increased cross-link density increased the hardness and strength of the ENR phase, which made it more difficult to become elongated to form microfibrils. When the tensile stress in the ENR phase is beyond the maximum support of the interfacial adhesion, the stretch breaking ENR finally “pulled out”, leaving irregular concavities as shown in Figure 13d. As a result, a further increase of DCP content corresponded to an indistinctive improvement in impact strength.

3. CONCLUSIONS

In this work, ENR-toughened PLA TPVs were successfully prepared through peroxide-induced dynamic vulcanization. Similar to that of our previous reported PLA/NR system, novel co-continuous phase morphology was also formed in PLA/ENR system. A remarkable brittle–ductile transition occurred at a 60:40 ratio of PLA/ENR, with an impact strength of 47 kJ/m², nearly 15 times that of neat PLA (3 kJ/m²). The improved impact toughness of TPVs mainly depended on the weight ratio, phase morphology, and DCP content. With an increasing of DCP content, excellent interfacial adhesions were achieved via interface reactions to form PLA-g-ENR copolymers, and a higher cross-link degree of ENR was realized. DCP also caused the slightly cross-linking and branching of PLA molecules. Morphological studies showed that the synergistic effect of improved interfacial adhesion, a netlike ENR continuous phase, and massive plastic deformations of the PLA matrix had significant improvement that impacted the toughness of TPVs.

AUTHOR INFORMATION

Corresponding Authors

*C. Xu e-mail: xuhuiyee@gxu.edu.cn.

*Y. Chen e-mail: cyl@scut.edu.cn. Tel: 02087110804. Fax: 02085293483.

Notes

The authors declare no competing financial interest.

REFERENCES

- (1) Reddy, M. M.; Vivekanandhan, S.; Misra, M.; Bhatia, S. K.; Mohanty, A. K. Biobased Plastics and Bionanocomposites: Current Status and Future Opportunities. *Prog. Polym. Sci.* **2013**, *38*, 1653–1689.
- (2) Liang, Y.; Yang, S.; Jiang, X.; Zhong, G.; Xu, J.; Li, Z. Nucleation Ability of Thermally Reduced Graphene Oxide for Polylactide: Role of Size and Structural Integrity. *J. Phys. Chem. B* **2015**, *119*, 4777–4787.
- (3) Madhavan Nampoothiri, K.; Nair, N. R.; John, R. P. An Overview of the Recent Developments in Polylactide (PLA) Research. *Bioresour. Technol.* **2010**, *101*, 8493–8501.
- (4) Mao, H.; Pan, P.; Shan, G.; Bao, Y. In Situ Formation and Gelation Mechanism of Thermoresponsive Stereocomplexed Hydrogels upon Mixing Diblock and Triblock Poly(Lactic Acid)/Poly(Ethylene Glycol) Copolymers. *J. Phys. Chem. B* **2015**, *119*, 6471–6480.
- (5) Zeng, J.; Li, K.; Du, A. Compatibilization Strategies in Poly(Lactic Acid)-Based Blends. *RSC Adv.* **2015**, *5*, 32546–32565.
- (6) Stoclet, G.; Seguela, R.; Lefebvre, J. M. Morphology, Thermal Behavior and Mechanical Properties of Binary Blends of Compatible Biosourced Polymers: Polylactide/Polyamide11. *Polymer* **2011**, *52*, 1417–1425.
- (7) Pongtanayut, K.; Thongpin, C.; Santawitee, O. The Effect of Rubber on Morphology, Thermal Properties and Mechanical Properties of PLA/NR and PLA/ENR Blends. *Energy Procedia* **2013**, *34*, 888–897.
- (8) Ishida, S.; Nagasaki, R.; Chino, K.; Dong, T.; Inoue, Y. Toughening of Poly(L-lactide) by Melt Blending with Rubbers. *J. Appl. Polym. Sci.* **2009**, *113*, 558–566.
- (9) Ojijo, V.; Ray, S. S.; Sadiku, R. Toughening of Biodegradable Polylactide/Poly(butylene Succinate-Co-Adipate) Blends Via in Situ Reactive Compatibilization. *ACS Appl. Mater. Interfaces* **2013**, *5*, 4266–4276.
- (10) Al-Ittry, R.; Lamnawar, K.; Maazouz, A. Improvement of Thermal Stability, Rheological and Mechanical Properties of PLA, PBAT and their Blends by Reactive Extrusion with Functionalized Epoxy. *Polym. Degrad. Stab.* **2012**, *97*, 1898–1914.
- (11) Zhang, L.; Xiong, Z.; Shams, S.; Yu, R.; Huang, J.; Zhang, R.; Zhu, J. Free Radical Competitions in Polylactide/Bio-Based Thermoplastic Polyurethane/Free Radical Initiator Ternary Blends and their Final Properties. *Polymer* **2015**, *64*, 69–75.
- (12) Chen, Y.; Xu, C.; Liang, X.; Cao, L. In Situ Reactive Compatibilization of Polypropylene/Ethylene-Propylene-Diene Monomer Thermoplastic Vulcanizate by Zinc Dimethacrylate via Peroxide-Induced Dynamic Vulcanization. *J. Phys. Chem. B* **2013**, *117*, 10619–10628.
- (13) Wu, H.; Tian, M.; Zhang, L.; Tian, H.; Wu, Y.; Ning, N. New Understanding of Microstructure Formation of the Rubber Phase in Thermoplastic Vulcanizates (TPV). *Soft Matter* **2014**, *10*, 1816–1822.
- (14) Liu, H.; Chen, F.; Liu, B.; Estep, G.; Zhang, J. Super Toughened Poly(Lactic acid) Ternary Blends by Simultaneous Dynamic Vulcanization and Interfacial Compatibilization. *Macromolecules* **2010**, *43*, 6058–6066.
- (15) Lu, X.; Wei, X.; Huang, J.; Yang, L.; Zhang, G.; He, G.; Wang, M.; Qu, J. Supertoughened Poly(Lactic acid)/Polyurethane Blend Material by in Situ Reactive Interfacial Compatibilization via Dynamic Vulcanization. *Ind. Eng. Chem. Res.* **2014**, *53*, 17386–17393.
- (16) Liu, H.; Song, W.; Chen, F.; Guo, L.; Zhang, J. Interaction of Microstructure and Interfacial Adhesion on Impact Performance of Polylactide (PLA) Ternary Blends. *Macromolecules* **2011**, *44*, 1513–1522.
- (17) Liu, G.; He, Y.; Zeng, J.; Li, Q.; Wang, Y. Fully Biobased and Supertough Polylactide-Based Thermoplastic Vulcanizates Fabricated by Peroxide-Induced Dynamic Vulcanization and Interfacial Compatibilization. *Biomacromolecules* **2014**, *15*, 4260–4271.
- (18) Ma, P.; Xu, P.; Liu, W.; Zhai, Y.; Dong, W.; Zhang, Y.; Chen, M. Bio-Based Poly(Lactide)/Ethylene-Co-Vinyl Acetate Thermoplastic Vulcanizates by Dynamic Crosslinking: Structure Vs. Property. *RSC Adv.* **2015**, *5*, 15962–15968.
- (19) Liu, G.; He, Y.; Zeng, J.; Xu, Y.; Wang, Y. In Situ Formed Crosslinked Polyurethane Toughened Polylactide. *Polym. Chem.* **2014**, *5*, 2530–2539.
- (20) Oyama, H. T. Super-Tough Poly(Lactic Acid) Materials: Reactive Blending with Ethylene Copolymer. *Polymer* **2009**, *50*, 747–751.
- (21) Lebarbé, T.; Grau, E.; Alfos, C.; Cramail, H. Fatty Acid-Based Thermoplastic Poly(Ester-Amide) as Toughening and Crystallization Improver of Poly(L-Lactide). *Eur. Polym. J.* **2015**, *65*, 276–285.
- (22) Kang, H.; Hu, X.; Li, M.; Zhang, L.; Wu, Y.; Ning, N.; Tian, M. Novel Biobased Thermoplastic Elastomer Consisting of Synthetic Polyester Elastomer and Polylactide by in Situ Dynamical Crosslinking Method. *RSC Adv.* **2015**, *5*, 23498–23507.
- (23) Bitinis, N.; Fortunati, E.; Verdejo, R.; Armentano, I.; Torre, L.; Kenny, J. M.; López-Manchado, M. Á. Thermal and Bio-Disintegration Properties of Poly(Lactic Acid)/Natural Rubber/Organoclay Nanocomposites. *Appl. Clay Sci.* **2014**, *93–94*, 78–84.
- (24) Bitinis, N.; Verdejo, R.; Cassagnau, P.; Lopez-Manchado, M. A. Structure and Properties of Polylactide/Natural Rubber Blends. *Mater. Chem. Phys.* **2011**, *129*, 823–831.
- (25) Wannapa, C.; Pamela, P.; Jean-Francois, P.; Varaporn, T. Bio-Based Diblock Copolymers Prepared From Poly(lactic Acid) and Natural Rubber. *J. Appl. Polym. Sci.* **2014**, *14146*–41436.
- (26) Chen, Y.; Yuan, D.; Xu, C. Dynamically Vulcanized Biobased Polylactide/Natural Rubber Blend Material with Continuous Cross-Linked Rubber Phase. *ACS Appl. Mater. Interfaces* **2014**, *6*, 3811–3816.
- (27) Chumeka, W.; Tanrattanakul, V.; Pilard, J.; Pasetto, P. Effect of Poly(Vinyl Acetate) on Mechanical Properties and Characteristics of Poly(Lactic Acid)/Natural Rubber Blends. *J. Polym. Environ.* **2013**, *21*, 450–460.
- (28) Jaratrotkamjorn, R.; Khaokong, C.; Tanrattanakul, V. Toughness Enhancement of Poly(Lactic Acid) by Melt Blending with Natural Rubber. *J. Appl. Polym. Sci.* **2012**, *124*, 5027–5036.
- (29) Juntuek, P.; Ruksakulpiwat, C.; Chumsamrong, P.; Ruksakulpiwat, Y. Effect of Glycidyl Methacrylate-Grafted Natural Rubber On Physical Properties of Polylactic Acid and Natural Rubber Blends. *J. Appl. Polym. Sci.* **2012**, *125*, 745–754.
- (30) Xu, K.; He, C.; Wang, Y.; Luo, Y.; Liao, S.; Peng, Z. Preparation and Characterization of Epoxidized Natural Rubber. *Adv. Mater. Res.* **2011**, *396–398*, 478–481.
- (31) Zhang, C.; Wang, W.; Huang, Y.; Pan, Y.; Jiang, L.; Dan, Y.; Luo, Y.; Peng, Z. Thermal, Mechanical and Rheological Properties of Polylactide Toughened by Epoxidized Natural Rubber. *Mater. Eng.* **2013**, *45*, 198–205.
- (32) Akbari, A.; Jawaid, M.; Hassan, A.; Balakrishnan, H. Epoxidized Natural Rubber Toughened Polylactic Acid/Talc Composites: Mechanical, Thermal, and Morphological Properties. *J. Compos. Mater.* **2014**, *48*, 769–781.
- (33) Zakaria, Z.; Islam, M. S.; Hassan, A.; Mohamad Haafiz, M. K.; Arjmandi, R.; Inuwa, I. M.; Hasan, M. Mechanical Properties and Morphological Characterization of PLA/Chitosan/Epoxydized Natural Rubber Composites. *Adv. Mater. Sci. Eng.* **2013**, *2013*, 1–7.
- (34) Bala, P.; Samantaray, B. K.; Srivastava, S. K.; Nando, G. B. Organomodified Montmorillonite as Filler in Natural and Synthetic Rubber. *J. Appl. Polym. Sci.* **2004**, *92*, 3583–3592.
- (35) Yuan, X.; Peng, Z.; Zhang, Y.; Zhang, Y. In Situ Preparation of Zinc Salts of Unsaturated Carboxylic Acids to Reinforce NBR. *J. Appl. Polym. Sci.* **2000**, *77*, 2740–2748.

- (36) Du, A.; Peng, Z.; Zhang, Y.; Zhang, Y. Effect of Magnesium Methacrylate on the Mechanical Properties of EVM Vulcanizate. *Polym. Test.* **2002**, *21*, 889–895.
- (37) Vennemann, N.; Bokamp, K.; Broker, D. Crosslink Density of Peroxide Cured TPV. *Macromol. Symp.* **2006**, *245–246*, 641–650.
- (38) Ouyang, W. Z.; Huang, Y.; Luo, H. J.; Wang, D. S. Preparation and Properties of Poly(Lactic Acid)/Cellulolytic Enzyme Lignin/PGMA Ternary Blends. *Chin. Chem. Lett.* **2012**, *23*, 351–354.
- (39) Yuan, D.; Xu, C.; Chen, Z.; Chen, Y. Crosslinked Bicontinuous Biobased Polylactide/Natural Rubber Materials: Super Toughness, "Net-Like"-Structure of NR Phase and Excellent Interfacial Adhesion. *Polym. Test.* **2014**, *38*, 73–80.
- (40) Wu, S. Phase Structure and Adhesion in Polymer Blends: A Criterion for Rubber Toughening. *Polymer* **1985**, *26*, 1855–63.
- (41) Wu, H.; Tian, M.; Zhang, L.; Tian, H.; Wu, Y.; Ning, N.; Chan, T. W. New Understanding of Morphology Evolution of Thermoplastic Vulcanizate (TPV) during Dynamic Vulcanization. *ACS Sustainable Chem. Eng.* **2015**, *3*, 26–32.
- (42) Yang, S.; Wu, Z.; Yang, W.; Yang, M. Thermal and Mechanical Properties of Chemical Crosslinked Polylactide (PLA). *Polym. Test.* **2008**, *27*, 957–963.
- (43) Salaeh, S.; Nakason, C. Influence of Modified Natural Rubber and Structure of Carbon Black On Properties of Natural Rubber Compounds. *Polym. Compos.* **2012**, *33*, 489–500.
- (44) Semba, T.; Kitagawa, K.; Ishiaku, U. S.; Hamada, H. The Effect of Crosslinking On the Mechanical Properties of Polylactic Acid/Polycaprolactone Blends. *J. Appl. Polym. Sci.* **2006**, *101*, 1816–1825.
- (45) Lin, T.; Guo, B. Curing of Rubber Via Oxa-Michael Reaction Toward Significantly Increased Aging Resistance. *Ind. Eng. Chem. Res.* **2013**, *52*, 18123–18130.
- (46) Maschio, G.; Bruni, C.; De Tullio, L.; Ciardelli, F. Analysis of the Molecular Weight Distribution (MWD) in Polymerization Processes: Contribution of Different Families of Active Sites to the MWD of Polyethylene Prepared Using Supported Transition Metal Catalysts. *Macromol. Chem. Phys.* **1998**, *199*, 415–421.